Int. J. Nano Dimens., 12 (4): 393-401, Autumn 2021

ORIGINAL ARTICLE

Design guidelines of InGaN nanowire arrays for photovoltaic applications

Imène Segmene[1], Yassine Sayad [1],, Nesrine Selatni[1], Abdelkader Nouiri[2]*

[1]LPMR Laboratory, Mohamed-Cherif Messaadia University, Souk-Ahras, 41000, Algeria
[2]LMSSEF Laboratory, Larbi Ben M'hidi University, Oum El-Bouaghi, 04000, Algeria

Received 13 June 2021, revised 14 July 2021, accepted 24 July 2021, available online 02 August 2021

Abstract

III-Nitride NanoWire array Solar Cells (NWSCs) combine the inherent properties of III-N semiconductors with waveguiding and confinement properties of nanowire arrays. In the present paper, some design guidelines of NWSCs made from Indium-Gallium-Nitride InGaN alloys are presented. Firstly, a detailed balance analysis was performed to show the importance of using InGaN materials to effectively convert the light to electricity, followed by an optical modelling to point out the advantages of using periodic nanowire arrays in designing solar cells. From the detailed balance analysis, it is expected that single junction solar cells made from In0.63Ga0.37N alloy result in the highest light-to-electricity conversion efficiency of 31%, and the Rigorous Coupled Wave Analysis RCWA simulations show that nanowire arrays made from $In_xGa_{1-x}N$ fractions (x values) ranging between 50 and 77% alloys may achieve efficiencies of more than 33%, with a maximum efficiency of 37.7% for In0.67Ga0.33N NW array. Substrate choice, array density and filling material impacts on device performance were also studied.

Keywords: *Detailed Balance Principle; InGaN Alloys; Nanowires; Optical Modelling; Solar Cell.*

How to cite this article

Segmene I, Sayad Y, Selatni N, Nouiri A. Design guidelines of InGaN nanowire arrays for photovoltaic applications. Int. J. Nano Dimens., 2021; 12(4): 393-401.

INTRODUCTION

Compound III-Nitride semiconductors (InN, GaN and AlN) and their alloys are widely used materials in optoelectronics fabrication of light-emitting diodes LEDs and laser diodes LDs emitting in visible and Ultra-Violet UV bands [1-3]. In photovoltaics, however, III-Nitrides are less used materials compared to other semiconductors (silicon, cadmium telluride, chalcopyrites,...) despite their potential to convert most of the solar spectrum to electricity [4] and their ability to withstand high-temperature and ionising radiation [5,6].

To build these devices, thin layers of III-nitrides are, usually, grown on foreign substrates (sapphire or silicon) with thicknesses limited by the high lattice mismatch which results in a high density of dislocations and strain induced polarisation.

On the other hand, in the last two decades, III-Nitride nanowire based photonic devices attract big attention owing to the ability of nanowires to be grown on foreign substrates, by various methods, without having to worry about lattice mismatch [7-11]. Furthermore, NanoWire array Solar Cells NWSCs present a significantly large effective surface area compared to planar cells for the same volume of matter and, hence, can present an enhanced light absorption and free carrier generation.

According to several recent research, the best experimentally achieved efficiencies of nanowire solar cells nowadays are, 13.8% for indium-phosphide InP NWSC [11] and 15.3% for gallium-arsenide GaAs NWSC [13], however, the III-Nitride based ones are still at lower efficiencies (with the best record of 2.73% [14]) and they have a longer way to go to meet the expected ambitions.

* Corresponding Author Email: *sayad.yassine@gmail.com, yassine.sayad@univ-soukahras.dz*

This work is licensed under the Creative Commons Attribution 4.0 International License.
To view a copy of this license, visit http://creativecommons.org/licenses/by/4.0/.

In fact, it is not only the semiconductor gap that may limit power conversion efficiency but also the existence of other sources of power losses in solar cells: thermalisation losses, losses by reflection / transmission (treated, in part, in this study), losses by recombination of charge carriers (radiative, by defect-related centers, at contacts). In this study, guidelines to optimal design of indium-gallium-nitride InGaN nanowire array solar cells were given. Starting with a detailed balance analysis, the importance of using InGaN alloys in photovoltaics was emphasized (next section), after that, full electromagnetic wave simulations of periodic arrays of vertically-aligned hexagonal nanowires were performed to show the impact of wires dimensions, substrate choice, array density and filling material on overall InGaN NWSC performance.

MATERIALS AND METHODS

PHOTOVOLTAIC POTENTIAL OF III-N MATERIALS

According to Shockley and Queisser detailed balance principle [15,16], which takes into account the energy gap of absorber material, it is expected that the efficiency limit of single junction solar cells under standard conditions (i.e. one sun illumination and 300°K) cannot exceed 31% [17] as it is shown in Fig. 1. Hence, it is expected that the solar cells made from indium nitride InN (with an energy gap of 0.675eV [18]) can result in higher efficiencies than gallium nitride GaN (3.435eV [19] and the aluminium-gallium nitride AlGaN alloys, whereas, the indium-gallium nitride InGaN alloys with intermediate energy gaps between that of InN and GaN materials matches best cell efficiencies region. In fact, the energy gap and related optical properties of InGaN alloys are still a matter of research works but, in general, the dependence of $In_xGa_{1-x}N$ alloys energy gap on indium element mole fraction, x, obeys to a rectified Vegard's law,

$$E_g^{InGaN} = x.E_g^{InN} + (1-x)E_g^{GaN} - b.x(1-x) \qquad (1)$$

Where the bowing factor b (quantify divergence to linear interpolation between E_g^{InN} and E_g^{GaN}) of unstrained Wurtzite InGaN films equals 1.65[19].

By applying equation (1), one can see that InGaN alloys with indium element mole fractions ranging from 53 to 73% can result in efficiencies of more than 30% (see inset graph in Fig. 1), with an efficiency limit, around 31%, for 0.63 as indium mole fraction x (corresponding energy gap of 1.3eV).

METHODS

In fact, Shockley and Queisser detailed balance principle only takes into account the absorber energy gap only, and cannot consider the optical

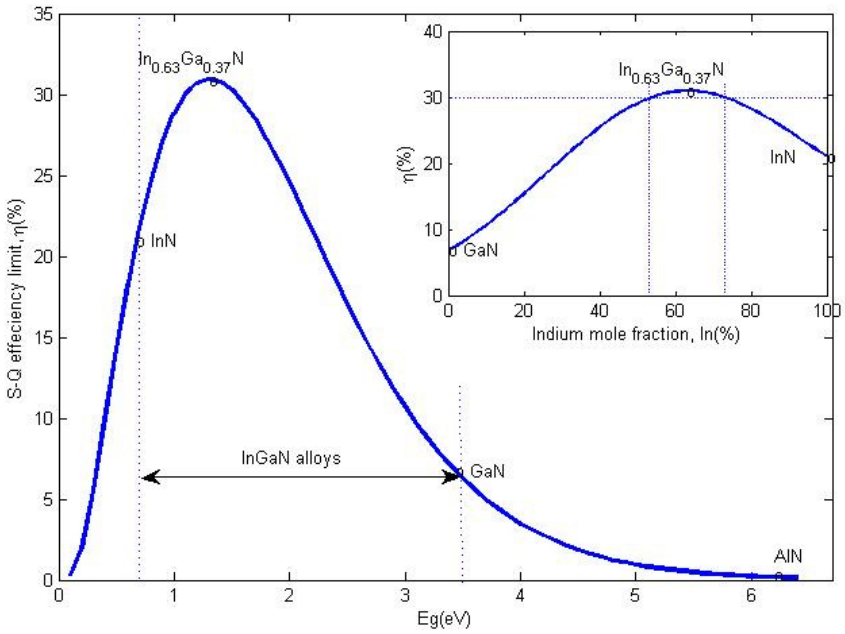

Fig. 1. Shockley-Queisser efficiency limit of single junction solar cells versus bandgap under one sun illumination.

losses (by reflection and/or transmission), the quantity of used matter nor device design in efficiency limit formulation [15]. Therefore, in order to assess light harvesting by periodic nanowire arrays, we need an appropriate optical modelling; and since the typical dimensions of nanowires and array periods (from few tens to few hundreds of nanometer) belong to the same order of magnitude of light wavelengths of interest (300-1000 nm) we need a full electromagnetic wave modelling of light inside and in the vicinity of the investigated device.

As a result of resolving the coupled Maxwell equations, the fractions of reflected R and transmitted T powers of a predefined incident light source (wavelength, orientation and polarisation) by the simulated device may be calculated. From which, we can deduce the fraction of the absorbed power (or absorptance, A) i.e. A=1-R-T.

The frequently used numerical methods in solving Maxwell equations are the Finite Difference (in time domain FDTD or in frequency domain FDFD), Finite Element method FEM and Rigorous Coupled Wave Analysis method RCWA (also called Fourier Modal Method FMM). Here, a scattering matrices formulation of RCWA, which is suitable to multilayer devices like solar cells were applied [20]. To perform RCWA calculations we, also, need for experimentally measured or reliable models of complex dielectric function DF, $\varepsilon(\lambda)=\varepsilon_1(\lambda)+i\varepsilon_2(\lambda)$, of the involved materials. But, unfortunately, there are neither enough data to cover all $In_xGa_{1-x}N$ alloys nor reliable models so far. In the next paragraphs, the available data of ordinary DF for some InGaN alloys measured by spectroscopic ellipsometry SE taken from the existing literature were used [19, 21-23].

In practice, the bottom-up growth approaches of InGaN nanowires using MOCVD or MBE systems result– in hexagonally shaped wires with equal sides [24-26] instead of uniform cylinders as he the case for many other semiconductors. Therefore, in subsequent RCWA simulations, periodic arrays (with period P) of hexagonally shaped nanowires with equal lengths L and diameters D (or sides S=D/2) were considered (as it is depicted in Fig. 2a). Then, in order to express the density of arrays, a filling factor *f* is defined as the ratio of nanowire

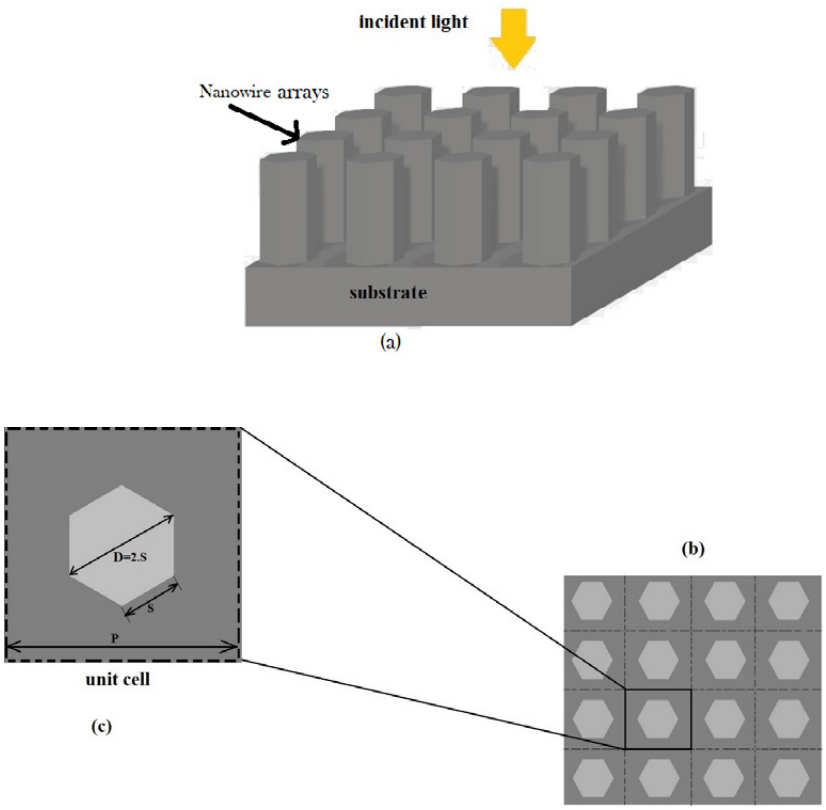

Fig. 2. Schematic of periodic nanowire array: (a) 3D view and (b)top view with emphasis to unit cell(c).

cross-section area to unit cell area (see Figs. 2 b-c),

$$f = \frac{3\sqrt{3}}{2}\left(\frac{S}{P}\right)^2 = \frac{3\sqrt{3}}{8}\left(\frac{D}{P}\right)^2 \quad (2)$$

Also, homogeneous illumination by transversely polarized T.E. electromagnetic waves was assumed throughout this study.

RESULTS AND DISCUSSION

FREELY STANDING InGaN NWs

In order to assess light confinement by $In_xGa_{1-x}N$ nanowire arrays as a function of indium mole fraction x of these alloys, square arrays of freely standing nanowires (without substrate) with same geometrical dimensions (period P=500nm, diameter D=2.S=250nm and length L=1µm) and different indium mole fractions ranging from gallium nitride GaN to indium nitride InN were considered. Exactly, the absorptance spectra (A) of $In_xGa_{1-x}N$ nanowire arrays with indium mole fraction (In/(In+Ga))×100 of 0, 20, 25, 30, 40, 50, 62, 67 ,77 and 100, with available dielectric function and energy gap data [19, 21-23] were calculated (see Fig.3). Fig. 3 shows that nanowire arrays made from InGaN alloys with indium fractions of more than 50% may present a high and broadband absorption i.e. A>0.75 for λ=300-800nm, and for longer wavelengths(λ>800nm) absorptance spectra were more broadened for NW arrays containing more indium element proportions.

On the other hand, by assuming an internal quantum efficiency of unity (i.e. number of absorbed photons equals the number of collected photo-carriers), it is possible to calculate an ultimate efficiency η_{max} and an ultimate short-circuit current J_{SCmax} from absorptance spectra (Fig. 3) using the following equations [15, 27],

$$\eta_{max} = \frac{\int_{300nm}^{\lambda_g} \frac{\lambda}{\lambda_g} A(\lambda) Ir_{AM1.5G}(\lambda) d\lambda}{\int_{300nm}^{4000nm} Ir_{AM1.5G}(\lambda) d\lambda} \quad (3)$$

$$Jsc_{max} = \int_{300nm}^{\lambda_g} \frac{q\lambda}{hc} A(\lambda) Ir_{AM1.5G}(\lambda) d\lambda = \frac{q\lambda_g}{hc} \eta_{max} \int_{300nm}^{4000nm} Ir_{AM1.5G}(\lambda) d\lambda \quad (4)$$

Where λ_g is gap wavelength, $Ir_{AM1.5G}$ is ASTM G-173 standard global solar irradiance AM1.5G [28]. q, h and c are electric charges, Planck's constant and velocity of light in vacuum, respectively.

Fig. 4 shows the calculated ultimate efficiencies (left y-axis) and ultimate short-circuit currents (right y-axis) versus indium mole fraction (obtained by applying equations (3) and (4)).

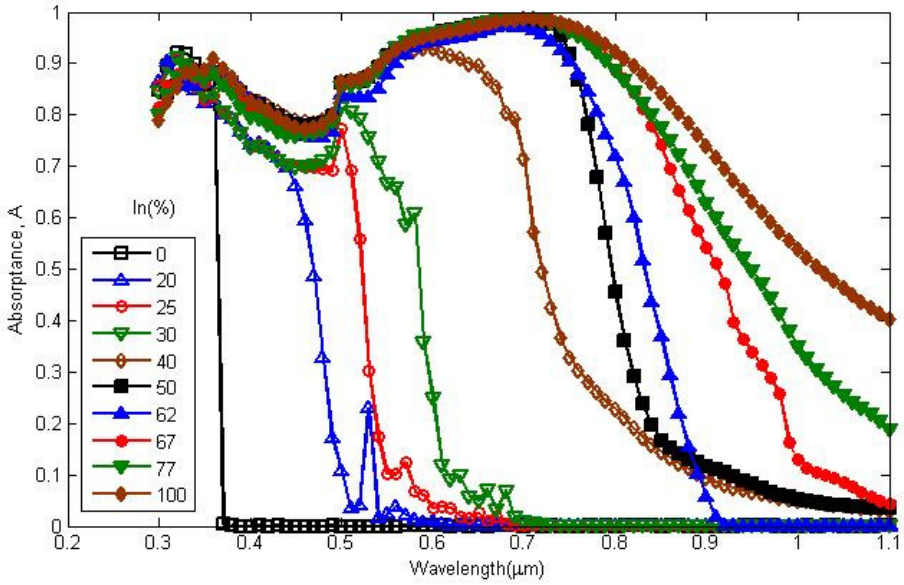

Fig. 3. Absorptance spectra of $In_xGa_{1-x}N$ NWAs (with period P=500nm, diameter D=2.S=250nm and length L=1µm) for different indium mole fractions, In(%).

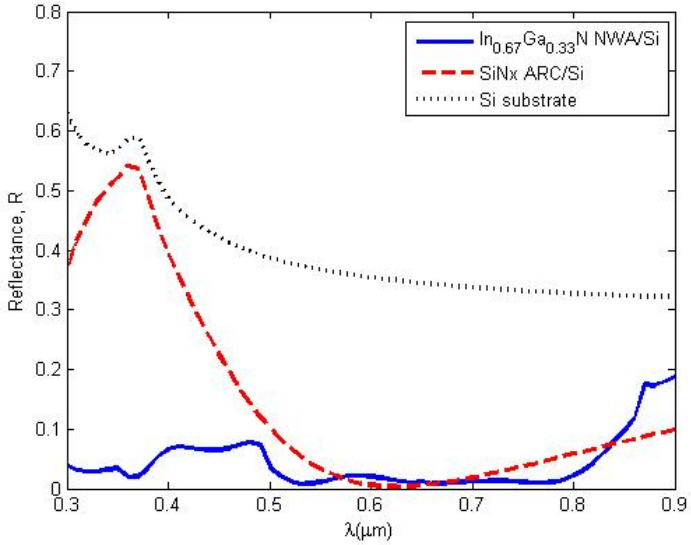

Fig. 4. Ultimate efficiencies (left y-axis) and ultimate short-circuit currents (right y-axis) of freely standing $In_xGa_{1-x}N$ nanowire arrays (P=500nm, D=250nm and L=1μm) versus indium element mole fraction.

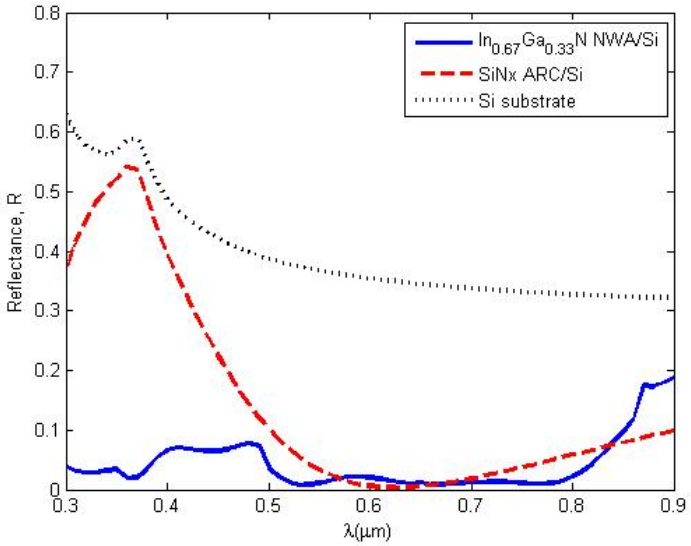

Fig. 5. Reflectance spectra of $In_{0.67}Ga_{0.33}N$ nanowire array (solid line) as well as SiNx ARC layer (dashed line) on silicon substrate, and of bare silicon substrate (dotted line).

While short-circuit current j_{SCmax} increases with the increase of In(%) until reaching a maximum of 36mA/cm^2 for InN NW array, efficiency η_{max} presents a maximum of 37.7% for $In_{0.67}Ga_{0.33}N$ NW array.

It is important to note, here, that this indium mole fraction (67%) is near to that predicted by the detailed balance analysis (i.e. 63%, see section 2).

InGaN NWs ON SILICON

The nature of used substrate in nanowires growth makes a big difference in terms of substrate contribution to total reflectance, especially, for low dense arrays and under the normal incidence of light. In practice, InGaN nanowire arrays were grown on sapphire, silicon or on costly bulk GaN substrates. From the photovoltaic point of view, growing InGaN NWs on the front surface of silicon

cells may, greatly, reduce-front surface reflectivity even in absence of the Anti-Reflection Coating (ARC) layer in the so-called black silicon solar cells [29].

Fig. 5 shows the calculated reflectance spectra of $In_{0.67}Ga_{0.33}N$ nanowire array NWA (solid line) (D=200nm, P=250nm and length L=1µm) along with silicon nitride SiNx Anti-Reflective Coating ARC layer of 75nm (dashed line), both on the bulky silicon substrate of 200µm. Reflectance spectra of the silicon substrate (dotted line) were, also, added for comparison. Here, dielectric function data of Si and SiNx were, respectively, taken from refs. [30, 31].

The obtained curves show very low reflections (less than 7 %) by the assumed NWA

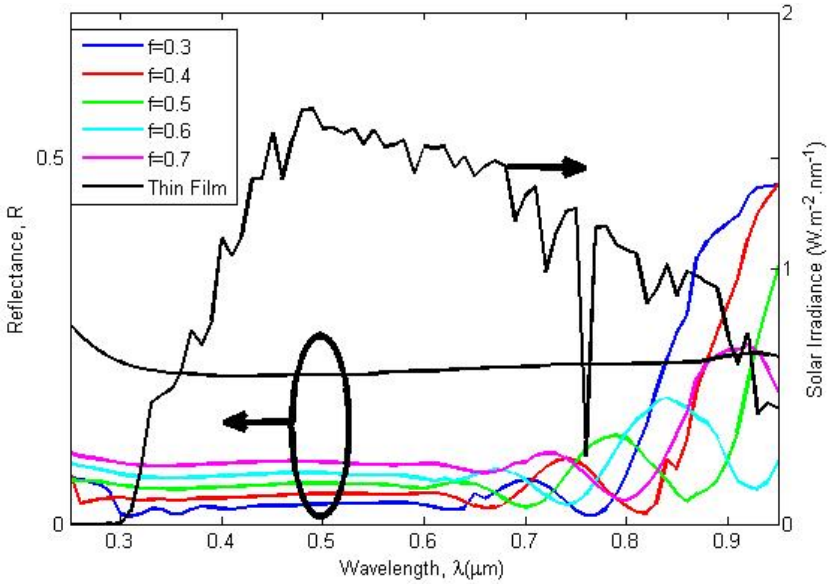

Fig. 6. Reflectance spectra of $In_{0.67}Ga_{0.33}N$ nanowire arrays on silicon versus filling factor (left y axis) and solar irradiance (right y axis).

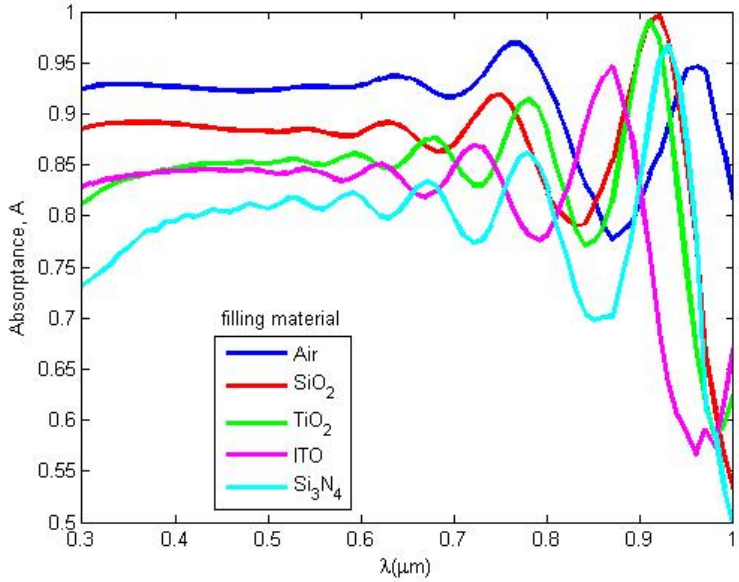

Fig. 7. Absorptance of $In_{0.67}Ga_{0.33}N$ NWA on Silicon in the presence of different filling materials.

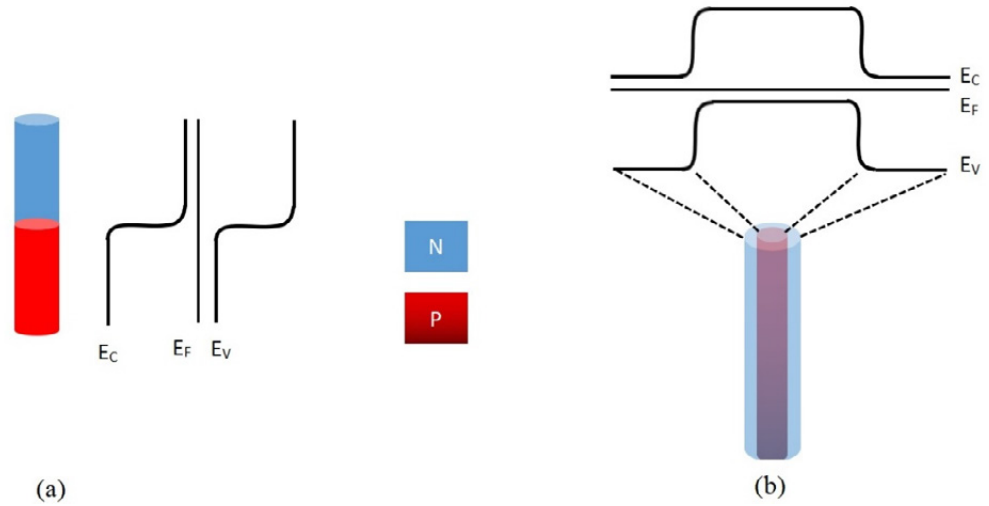

Fig. 8. PN junction nanowires with corresponding schematic band diagrams: (a) axial junction and radial core/shell junction (b).

for a broadband of wavelengths (300-800nm) compared to the ARC layer designed to work well for a unique wavelength (here, 600nm).

In order to deepen the precedent analysis and to check the influence of InGaN nanowires density on frontal reflectance of the silicon cell, reflectance spectra of $In_{0.67}Ga_{0.33}N$ nanowire arrays on silicon for filling factors *f* ranging from 0.3 to 0.7, were calculated (by maintaining a constant diameter D=200nm and length L=1µm, and changing period P to meet desired *f* values). Fig. 6 shows the obtained spectra of the NWAs as well as of an $In_{0.67}Ga_{0.33}N$ thin film of 1µm (corresponding to *f*=1). It is clear that all NWAs ensure low reflectance for broadband of wavelengths ranging from 300 to 800nm where the major part of solar irradiance exists(right y axis in Fig.6), and the better results may be guaranteed by less dense arrays (lower *f*).

On the other hand, the medium surrounding nanowires consolidates array morphology and plays a crucial role in light confinement and charge carriers transport. Thus, it is important to compare absorptance properties of the InGaN NWAs in the presence of different filling materials. Therefore, absorptance spectra of similar $In_{0.67}Ga_{0.33}N$ NWAs (P=500nm, D=200nm and L=1µm) on silicon filled by different dielectric materials (silicon dioxide SiO_2, titanium dioxide TiO_2, indium-tin-oxide In_2O_3-SnO_2 and silicon nitride Si_3N_4) were calculated, as it is shown in Fig. 7. All these materials have low absorptance in the wavelength domain of interest (i.e. 300<λ<1000nm) and are widely used in silicon photovoltaics.

Generally, the largest refractive index gradient (between nanowires and surrounding medium) ensures the best confinement of the light. This is the case of air (blue line) but this is not a practical situation since for some materials, one needs to strengthen the standing wires and, probably, to conduct charge carriers. Among the four materials, silicon dioxide (red line) may be the best choice since it results in less absorption losses if we do not need conductive material (for instance, in the case of nanowires with axial junction (see Fig. 8(a)) where charge carriers were to be extracted at wire terminals), whereas, the use of conductive material like ITO (magenta line), with more optical losses, is necessary if some conductive materials are needed (e.g. in the case of core/shell radial p-n junction nanowires (see Fig. 8(b))).

CONCLUSION

Semiconductor nanowire arrays are one of the promising ways to implement next generation solar cells through reducing optical losses and increasing carrier collection efficiency. In this study, detailed balance analysis and optical modelling were combined to outline the main factors to be considered in the design of III-Nitride based NanoWire array Solar Cells NWSC.

By applying the detailed balance principle, the photovoltaic potential is shown for the $In_xGa_{1-x}N$ alloys among other III-nitrides, especially, the indium rich ones, and the best efficiency of single junction solar cell, i.e. 31%, may be achieved using $In_{0.63}Ga_{0.37}N$ alloy.

CC BY

On the other hand, the Rigorous Coupled Wave Analysis RCWA simulations of freely standing (without substrate) and periodic $In_xGa_{1-x}N$ nanowire arrays show that arrays made from $In_xGa_{1-x}N$ alloys with indium element mole fraction, In(%), of more than 50% present a high and broadband absorptance, and ultimate efficiencies of more than 33% that may be achieved with mole fractions between 50 and 77% (with a maximum of 37.7% for $In_{0.67}Ga_{0.33}N$ based NWSC).

Then, advantages of growing InGaN nanowire arrays on silicon substrate (or cell) were identified. Simulations showed that absorption properties of InGaN nanowire arrays strongly depend on array density (low dense nanowire arrays NWA on silicon achieves lower reflection than dense ones). The choice of array filling materials (conductive or not) depends on junction type (radial or axial), but it, in all cases, reduces array absorptance.

DECLARATION OF INTERESTS

Authors have no conflict of interest.

AUTHOR CONTRIBUTIONS

Numerical modelling: Segmene I., Sayad Y. and Selatni N.

Writing & analysis: Sayad Y. and Nouiri A.

All authors have read and agreed to the submitted version of the manuscript.

ACKNOWLEDGEMENTS

We would like to express our special thanks of gratitude to Professor Rüdiger Goldhahn (Magdeburg, Germany) for providing us with some experimental data on the complex dielectric function and related documents.

REFERENCES

[1] Beeler M., Trichas E., Monroy E., (2013), III-nitride semiconductors for intersubband optoelectronics: A review. *Semiconduc. Sci. Technol.* 28: 074022.

[2] Razeghi M., (2011), III-nitride optoelectronic devices: From ultraviolet toward terahertz. *IEEE Photonics J.* 3: 263-267.

[3] Aran S., Liu X., Mi Z., (2013), Review of recent progress of III-nitride nanowire lasers. *J. Nanophoton.* 7: 1-28.

[4] Toledo N. G., Mishra U. K., (2012), InGaN solar cell requirements for higheciency integrated III-nitride/non-III-nitride tandem photovoltaic devices. *J. Appl. Phys.* 111: 114505.

[5] Sequeira M. C., Mattei J.-G., Vazquez H., Djurabekova F. , Nordlund K., Monnet I., Mota-Santiago P., Kluth P., Grygiel C., Zhang S., (2021), Unravelling the secrets of the resistance of GaN to strongly ionising radiation, *Communic. Phys*. 4:1-8.

[6] Chiamori H. C., Hou M., Chapin C. A., Shankar A., Senesky D. G., (2014), Characterization of gallium nitride microsystems within radiation and high-temperature environments, in: H. R. Shea, R. Ramesham (Eds.), Reliability, Packaging, Testing, and Characterization of MOEMS/MEMS, Nanodevices, and Nanomaterials XIII. *Int. Soc. Optics Photon. SPIE*. 8975: 42-49.

[7] Zhao C., Alfaraj N., Chandra Subedi R., Liang J. W., Alatawi A. A., Alhamoud A. A., Ebaid M., Alias M. S., Ng T. K., Ooi B. S., (2018), III-nitride nanowires on unconventional substrates: From materials to optoelectronic device applications. *Prog. Quant. Electron.* 61: 1-31.

[8] Sun H., Li X., (2019), Recent advances on III-nitride nanowire light emitters on foreign substrates - toward flexible photonics. *Phys. Status Solidi (A)* 216: 1800420.

[9] Shabannia R., (2019), Fast UV detection by Cu-doped ZnO nanorod arrays chemically deposited on PET substrate. *Int. J. Nano Dimens.*10: 313-319.

[10] Wang Z. L., (2003), Nanowires and nanobelts: Materials, properties and devices. Volume 1: Metal and Semiconductor Nanowires. Springer Science & Business Media.

[11] Aravindh S. A., Xin B., Mitra S., Roqan I. S., Najar A., (2020), GaN and InGaN nanowires prepared by metal-assisted electroless etching: Experimental and theoretical studies. *Results in Phys.* 19: 103428.

[12] Wallentin J., Anttu N., Asoli D., Human M., Aberg I., Magnusson M. H., Siefer G., Fuss-Kailuweit P., Dimroth F., Witzigmann B., Xu H. Q., Samuelson L., Deppert K., Borgström M. T., (2013), InP nanowire array solar cells achieving 13.8% eciency by exceeding the ray optics limit. *Science.* 339: 1057-1060.

[13] Aberg I. , Vescovi G., Asoli D., Naseem U., Gilboy J. P., Sundvall C., Dahlgren A., Svensson K. E., Anttu N., Björk M. T., Samuelson L., (2016), A GaAs nanowire array solar cell with 15.3% effciency at 1 sun. *IEEE J. Photovolt.* 6: 185-190.

[14] Tang Y. B., Chen Z. H., Song H. S., Lee C. S., Cong H. T., Cheng H. M., Zhang W. J., Bello I., Lee S. T., (2008), Vertically aligned p-type singlecrystalline GaN nanorod arrays on n-type si for heterojunction photovoltaic cells. *Nano Letters.* 8: 4191-4195.

[15] Shockley W., Queisser H. J., (1961), Detailed balance limit of eciency of p-n junction solar cells. *J. Appl. Phys*. 32: 510-519.

[16] Green M., (2003), Third generation photovoltaics, Springer-Verlag Berlin Heidelberg.

[17] Sayad Y., (2016), Photovoltaic potential of III-nitride based tandem solar cells. *J. Science: Adv. Mater. Dev.* 1: 379-381.

[18] Goldhahn R., Schely P., (2007), Roppischer M., Ellipsometry of InN and related alloys, CRC Press, Ch. 9 : 52.

[19] Sakalauskas E., Tuna Ö., Kraus A., Bremers H., Rossow U., Giesen C., Heuken M., Hangleiter A., Gobsch G., Goldhahn R., (2012), Dielectric function and bowing parameters of InGaN alloys. *Physica Status Solidi (B)*. 249: 485-488.

[20] Rumpf R. C., (2011), Improved formulation of scattering matrices for semianalytical methods that is consistent with convention. *Prog. In Electro Magnet. Res. B*. 35: 241-261.

[21] Schley P., Goldhahn R., Winzer A. T., Gobsch G., Cimalla V., Ambacher O., Rakel M., Cobet C., Esser N., Lu H., Scha W. J., (2006), Transition energies and stokes shift analysis for In-rich InGaN alloys. *Physica Status Solidi (B).* 243: 1572-1576.

[22] Goldhahn R., Buchheim C., Schley P., Winzer A. T., Wenzel

H., (2007), Optical constants of bulk nitrides, Wiley Weinheim, Ch. 5: 95-115.
[23] Kazazis S., Papadomanolaki E., Androulidaki M., Kayambaki M., Iliopoulos E., (2018), Optical properties of InGaN thin films in the entire composition range. *J. Appl. Phys.* 123: 125101.
[24] Park J.-H., Nandi R., Sim J.-K., Um D.-Y., Kang S., Kim J.-S., Lee C.-R., (2018), A III-nitride nanowire solar cell fabricated using a hybrid coaxial and uniaxial InGaN/GaN multi quantum well nanostructure. *RSC Adv*. 8: 20585-20592.
[25] Ra Y.-H., Lee C.-R., (2019), Understanding the p-type GaN nanocrystals on InGaN nanowire heterostructures. *ACS Photonics.* 6: 2397-2404.
[26] Schuster F., Weiszer S., Hetzl M., Winnerl A., Garrido J. A., Stutzmann M., (2014), Infuence of substrate material, orientation, and surface termination on GaN nanowire growth. *J. Appl. Phys.* 116: 054301.
[27] Lin C., Povinelli M. L., (2009), Optical absorption enhancement in silicon nanowire arrays with a large lattice constant for photovoltaic applications. *Opt. Express.* 17: 19371-19381.
[28] National Renewable Energy Laboratory, USA, https://www.nrel.gov/, (Accessed, June 2021).
[29] Haggren T., Khayrudinov V., Dhaka V., Jiang H., Shah A., Kim M., Lipsanen H., (2018), III-V nanowires on black silicon and low-temperature growth of self-catalyzed rectangular InAs NWs. *Scientic Reports.* 8: 1-9.
[30] Aspnes D. E., Studna A. A., (1983), Dielectric functions and optical parameters of Si, Ge, GaP, GaAs, GaSb, InP, InAs, and InSb from 1.5 to 6.0 eV. *Phys. Rev. B.* 27: 985-1009.
[31] Vogt M. R., (2015), Development of physical models for the simulation of optical properties of solar cell modules, Ph.D. thesis, Dissertation, Gottfried Wilhelm Leibniz Universitat Hannover, Hannover.

CC BY